Optimal Transmission Power and Controller Design for Networked Control Systems Under State-Dependent Markovian Channels

Bin Hu, *Member, IEEE*, and Tua A. Tamba

***Abstract*—This article considers a codesign problem for industrial networked control systems to ensure both stability and efficiency properties of such systems. This problem is particularly challenging due to the fact that wireless communications in industrial environments are not only subject to shadow fading, but also stochastically correlated with their surrounding environments. This article first introduces a novel state-dependent Markov channel (SD-MC) model that explicitly captures the *state-dependent features* of industrial wireless communication systems by defining the proposed model's transition probabilities as a function of both environments' states and transmission power. Under the SD-MC model, sufficient conditions on *Maximum Allowable Transmission Interval* are presented to ensure both *asymptotic stability in expectation* and *almost sure asymptotic stability* properties of a nonlinear control system with *state-dependent fading channels*. Based on these stability conditions, the codesign problem is then formulated as a constrained polynomial optimization problem (CPOP), which can be efficiently solved using semidefinite programming methods for the case of a two-state SD-MC model. The solutions to such a CPOP represent optimal control and power strategies that optimize the average expected joint costs in an infinite time horizon while respecting the stability constraints. For a general SD-MC model, this article further shows that suboptimal solutions can be obtained from linear programming formulations of the considered CPOP. Simulation results are given to illustrate the efficacy of the proposed codesign scheme.**

***Index Terms*—Almost sure asymptotic stability, constrained polynomial optimization, maximum allowable transmission interval (MATI), state-dependent Markovian channel.**

I. Introduction

A. Background and Motivation

Over the past couple of decades, wireless communication technologies have evolved rapidly and became ubiquitous in modern society. For instance, wireless communication protocols such as WirelessHart and WiMAX [1], [2] are considered among the important components that help improve modern industrial automation and build efficient, safe, and reconfigurable industrial automation systems.

Building a safe and efficient industrial networked control system (NCS) remains challenging because wireless communication channels in highly dynamic industrial environments are inherently unreliable and often subject to *shadow fading* phenomenon.

Such a phenomenon may seriously compromise system stability and performance as it causes significant degradation on the quality of communication links. The *shadow fading* effect is also known to be correlated to moving objects/machineries in industrial environments [2]–[5]. This thus gives rise to the needs for NCS channel modeling approach as well as assuring the stability and long-term efficiency of industrial automation systems. This article proposes a novel *State-Dependent Markov Channel* (SD-MC) model that specifically incorporates the impact of external environments (e.g., moving objects) on the channel conditions, and then develops a codesign formalism that ensures both stability and efficiency for the NCS.

B. Related Work

This section mainly reviews existing works related to 1) wireless channel modeling in industrial environments and 2) codesign methods for communication and control systems. For other related topics, interested readers are encouraged to refer to excellent surveys in [6] and [7].

Recent studies have shown that radio communication in industrial environments often exhibits *shadow fading* effect that is statistically dependent on the environment's various states and dynamics (large metal objects, moving machineries, and vehicles) [3], [5], [8]. Such *state-dependent features* prevent the use of conventional channel models such as Markov chain [9] or identically distributed independent process (i.i.d.) to capture communication channel dynamics [2], [4].

Several works have thus developed effective channel models that correlate the temporal variations of the channel conditions with the states of external environment in different industrial settings. In [5], [8], [10], a network state process was modeled by a Markov chain to characterize the *shadow fading* effects under a finite set of configurations. The state-dependent feature of wireless channels was modeled by the probability of packet losses as a function of the network state process. Other channel models were focused on the correlation between fading statistics and the movements of industrial objects/machines [3], [4], [11]. Qin *et al.* [4] proposed an impulse response framework to model the temporal fading effects in capturing nearby moving objects. Channel models combining multiple probability distributions were used in [2]–[4], [11]–[13] to capture sudden changes on fading statistics that were observed during extensive channel measurements in various industrial environments.

The SD-MC model proposed in this article is different from the aforementioned models in two aspects. First, the works in [5] and [8] model the external environment (i.e., a moving vehicle) as a (semi)-Markov chain and assume that the moving vehicle cannot be controlled. This article removes such uncontrollability assumptions and models the external environment as a Markov Decision Process (MDP). Second, the models adopted in [5], [8], [10] are confined to packet-drop channels

Manuscript received 15 March 2022; accepted 3 June 2022. Date of publication 10 June 2022; date of current version 27 September 2022. This work was supported by the National Science Foundation under Grant IIS-2007386, and in part by the Kemendikbudristek of Indonesia under the Fundamental Research Grant 2022. Recommended by Associate Editor N. Van De Wouw. *(Corresponding author: Bin Hu.)*

Bin Hu is with the Department of Engineering Technology, Old Dominion University, Norfolk, VA 23529 USA (e-mail: binhu.complicated@gmail.com).

Tua A. Tamba is with the Department of Electrical Engineering, Parahyangan Catholic University, Bandung 40141, Indonesia (e-mail: ttamba@unpar.ac.id).

Color versions of one or more figures in this article are available at https://doi.org/10.1109/TAC.2022.3181758.

Digital Object Identifier 10.1109/TAC.2022.3181758

0018-9286 © 2022 IEEE. Personal use is permitted, but republication/redistribution requires IEEE permission.
See https://www.ieee.org/publications/rights/index.html for more information.

Authorized licensed use limited to: University of Houston. Downloaded on October 03,2022 at 15:45:04 UTC from IEEE Xplore. Restrictions apply.

that ignore quantization effects. Here, we consider a generalized SD-MC model that takes into account the presence of time varying data rates.

As an effective means to mitigate channel fading effects, power control has been well studied in wireless communication community [14]. From NCS design perspective, it is important to further ensure both system stability and efficiency of the whole industrial system. These thus suggest that a joint design of power and control strategies must be considered. In regard of this, numerous codesign results were developed to design optimal controller [15]–[20] or state estimator [8], [21]–[25] for NCSs by incorporating impacts that fading channels have on the design processes. Regarding the codesign of optimal state estimator and transmission power, the works in [5], [8], [21]–[25] have shown that optimal estimation can be achieved using Kalman filters whose structural design is independent of the used wireless communication channels, whereas the optimal power policies take the form of functions of the channel states and the innovation error of the Kalman filter. For the codesign of optimal controller, the main ideas in prior works are basically that of applying the so-called separation principle, where the optimal design of communication and control strategies can be separated by assuming that the two are independent from each other. Such an assumption, however, has limited applicability in complex industrial environments, where the communication and control parts of the NCS are tightly coupled with the presence of *state-dependent fading channels*. Compared with existing results, the unique feature of the work presented in this article is the incorporation of mutual interaction between the communication and control systems into the codesign process via the proposed SD-MC model. By exploring such state-dependent features, this article shows that the resulting optimal codesign strategies are more robust and efficient against various levels of *shadow fading* than conventional methods.

This article extends our preliminary results in [26] in three main parts. First, this article includes a new stability result for a weaker notion of *asymptotic stability in expectation* (ASE) by using a less conservative Assumption 4.1. Second, a linear program-based approximation method is proposed to provide tractable and computationally efficient solutions for the codesign problem. Third, a nonlinear robotic arm system with more simulation results is presented to further validate and demonstrate advantages of the proposed codesign method.

C. Contributions

The main contributions of this article are summarized as follows:

1) A proposal of a novel SD-MC model that explicitly captures the dependency between channel states, controlled external environments, and transmission power. In particular, the incorporation of *state-dependent features* in the proposed SD-MC model generalizes the conventional Markov chain and i.i.d. models.
2) Based on the proposed channel model, this article then derives sufficient conditions on MATI that assure ASE and *almost sure asymptotic stability* (ASAS) of a nonlinear NCS. In particular, this article shows that the derived sufficient conditions on MATI generalize existing results in [27] through the incorporation of the *state-dependent* properties in the conditions.
3) Using the derived MATI constraints, this article then proposes a constrained polynomial optimization problem (CPOP) formulation to solve the codesign problems. Under the proposed codesign problem, system stability is assured by imposing the derived sufficient conditions as hard constraints in the CPOP formulation. The solutions to the CPOP thus represent optimal control and transmission power policies that minimize an average joint costs for both communication and control systems.

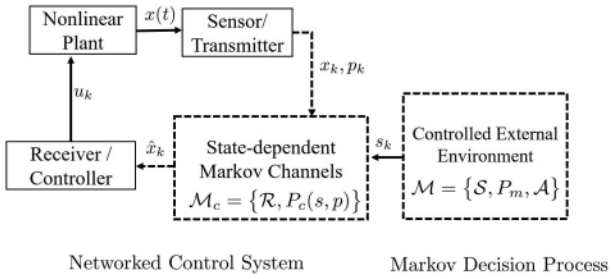

Fig. 1. Nonlinear NCS with SD-MC framework.

4) This article further shows that the formulated CPOP can be efficiently solved using SDP methods if a two-state Markovian channel model is considered. For a general Markovian channel model, the formulated CPOP can be approximated as linear programing (LP) problems whose solutions lead to suboptimal codesign strategies.

The rest of this article is organized as follows. The system framework is described in Section II, followed by problem formulation in Section III. The main results in terms of sufficient conditions on MATI and optimal codesign strategies are provided in Section IV. Simulation results are shown in Section V. Finally, Section VI concludes this article.

Notations: Throughout this article, let $\mathbb{R}, \mathbb{Z}$ denote the sets of real and integer numbers, respectively, and $\mathbb{R}_{\geq 0}, \mathbb{Z}_{\geq 0}$ denote their nonnegative counterparts. Let $\mathbb{R}^n$ and $\mathbb{R}^{n\times m}$ denote the n-dimensional real vector space and matrix of dimension $n \times m$, respectively. For a vector $x \in \mathbb{R}^n$, let $|x| = \max_i |x_i|$ denote its infinity norm, where x_i is the ith element of the vector and $1 \leq i \leq n$. For a matrix $A \in \mathbb{R}^{n\times m}$, let $|A| := \|A\|_\infty = \max_{1\leq i\leq m} \sum_{j=1}^{n} |a_{ij}|$ denote its infinity norm. A real matrix $A \in \mathbb{R}^{n\times n}$ is positive (semi)-definite, i.e., $A \succeq 0$, if $x^T A x \geq 0, \forall x \in \mathbb{R}^n$.

II. System Framework

The NCS system framework considered in this article is shown in Fig. 1, and consists of a *nonlinear plant*, a SD-MC $\mathcal{M}_c$, a *remote controller*, and *external environment* modeled by MDP $\mathcal{M}$.

1) Nonlinear Plant: The nonlinear plant dynamics are modeled by an ODE

$$\dot{x} = f(x, u) \tag{1}$$

where $x \in \mathbb{R}^{n_x}$ is the plant/system state that is directly measurable by the sensor and $u \in \mathbb{R}^{n_u}$ is the system input that is generated by a remote controller. The system vector fields are governed by a nonlinear function $f : \mathbb{R}^{n_x} \times \mathbb{R}^{n_u} \to \mathbb{R}^{n_x}$ that is locally Lipschitz with respect to x. In this article, we assume that the system state x can not be accessed directly by the controller, and thus must be transmitted through a wireless communication channel.

2) Sensor and Transmitter: The system state x is first preprocessed by a *sensor/transmitter* module before the transmission. This article considers both the sampling and quantization effects on x. Specifically, let $\{t_k\}_{k=0}^{\infty}$ be a sequence of sampling time instants with $t_k < t_{k+1}$, and $x_k := x(t_k)$ be the sampled state value at time instant t_k. The sampled state $x(t_k)$ is then encoded by one of a finite number of symbols that are constructed based on a dynamic quantization scheme [28]. Such a dynamic quantization scheme maps the sampled state $x \in \mathbb{R}^{n_x}$ into the index of a finite number of symbols. Specifically, let $R \in \mathbb{N}$ denote the number of bits used to construct the symbol such that the sequence of the symbols is labeled as $\mathcal{S} = \{1, 2, \ldots, 2^R\}$ with a total number of 2^R. The way of using such symbols to encode the state information $x(t_k)$ is by constructing a dynamic quantizer that is

Authorized licensed use limited to: University of Houston. Downloaded on October 03,2022 at 15:45:04 UTC from IEEE Xplore. Restrictions apply.

able to track the evolution of $x(t_k)$ at each transmission instant. The quantizer is defined as a tuple $\mathcal{Q} = (\mathcal{S}, q(\cdot), \xi)$, where $q(\cdot) : \mathbb{R}^{n_x} \to \mathcal{S}$ is a quantization function, which maps the system state into a symbol, while $\xi \in \mathbb{R}_{\geq 0}$ is an auxiliary variable defining the size of quantization regions.

A typical approach to implement the quantizer $\mathcal{Q}$ is based on the construction of a hybercubic box which evolves dynamically to contain and track the state x. To demonstrate the mechanism of such a box-based dynamic quantizer, suppose a hypercubic box is constructed at time instant t_k. Let $\hat{x}(t_k)$ and $2\xi(t_k)$, respectively, denote the center and the size of such a box. Then, the box is divided equally into 2^R smaller sub-boxes with each sub-box being labeled as one of the symbols in $\mathcal{S}$. Among all the symbols, let $q(x) \in \mathcal{S}$ denote the symbol (sub-box) that contains the state x. The center of that sub-box, $\hat{x}(t_k^+)$, is then used as an updated estimate of the state x at time instant t_k. Thus, the hyper-cubic box may then be updated with a new center of $\hat{x}(t_k^+)$ and a new size of $\xi(t_k^+) = \xi(t_k)/2^R$. The symbol representing this updated hybercubic is transmitted through the wireless communication channel. The dynamics of such a quantizer are modeled by

$$\hat{x}(t_k^+) = h(k, q(x(t_k)), \hat{x}(t_k), \xi(t_k), R_k) \tag{2a}$$

$$\xi(t_k^+) = \frac{\xi(t_k)}{2^{R_k}} \tag{2b}$$

where R_k is the number of bits available at time instant t_k that is correlated with the wireless channel conditions. As discussed in prior work [28], within each time interval $[t_k, t_{k+1}), \forall k \in \mathbb{Z}_{\geq 0}$, the size of the hypercubic box needs to be propagated to ensure the containment of the actual state x in the constructed box. Specifically, the following differential equation is used to characterize the evolution of the box size over time

$$\dot{\xi}(t) = g_\xi(\xi), \forall t \in [t_k, t_{k+1}). \tag{3}$$

In this article, we assume that the encoder and decoder are synchronized by a noiseless feedback channel so that both encoder and decoder can use equations (2) and (3) to track the system state x.

3) Remote Controller: Using the dynamic quantizer $\mathcal{Q}$, this article considers a model-based remote controller that maintains a "copy" of the plant dynamics in (1) defined as follows:

$$\dot{\hat{x}} = f(\hat{x}, u)$$

$$u = \kappa(\hat{x}), \forall t \in [t_k, t_{k+1}) \tag{4}$$

with initial state $\hat{x}(t_k) = \hat{x}(t_k^+)$. The control function $\kappa(\cdot) : \mathbb{R}^{n_x} \to \mathbb{R}^{n_u}$ is a "nominal" controller selected to stabilize the dynamics in (4) without considering the network effect.

Based on system dynamics in (1), the dynamic quantizer in (2) and (3), and the remote controller in (4), the closed-loop system can be characterized as a stochastic hybrid system (SHS) defined as follows:

$$\dot{x} = \tilde{f}(x, e) \tag{5a}$$

$$\dot{e} = g_e(x, e) \tag{5b}$$

$$\dot{\xi} = g_\xi(\xi), \forall t \in (t_k, t_{k+1}) \tag{5c}$$

and

$$e(t_k^+) = J_e(k, x(t_k), e(t_k), \xi(t_k), R_k) \tag{6a}$$

$$\xi(t_k^+) = J_\xi(\xi(t_k), R_k), \forall k \in \mathbb{Z}_{\geq 0} \tag{6b}$$

where $e := x - \hat{x}$ denotes the estimation error and $\tilde{f}(x, e) = f(x, \kappa(x - e))$, $g_e(x, e) = f(x, \kappa(x - e)) - f(x - e, \kappa(x - e))$, $J_e(k, x(t_k), e(t_k), \xi(t_k), R_k) = x(t_k) - h(k, q(x(t_k)), x(t_k) - e(t_k), \xi(t_k), R_k)$, and $J_\xi = \xi(t_k)2^{-R_k}$. Equation (5) models continuous dynamics of the closed loop system while (6) captures system's stochastic jump behavior induced by the time varying data rate of R_k.

4) Controlled External Environments and SD-MC Models: The industrial environment consisting of moving vehicles or machines is modeled by a MDP $\mathcal{M}_{\text{env}} = \{S, s_0, A, Q\}$ where $S = \{s_i\}_{i=1}^{M_s}$ is a finite set of environment states with initials s_0, $A = \{a_i\}_{i=1}^{M_a}$ is a finite set of actions, and $Q = \{q(s|s,' a)\}_{s,s' \in S, a \in A}$ is a transition matrix governing dynamics of the environment. Taking a forklift vehicle operating in manufacturing factory as an example, the state set S in MDP represents a partition of the factory floor on which the forklift vehicle operates. With a selected action $a \in A$, the vehicle moves from one region s' to another s following a transition probability $q(s|s', a)$. Under the MDP model, this article emphasizes the *state-dependent* property of wireless communication channels, where the quality of wireless links is affected by the state/region in which the forklift vehicle is located. The link quality is measured by a time varying data rate selected from a finite set $\mathcal{R} = \{r_1, r_2, \ldots, r_{M_R}\}$.

Let a sequence $\mathcal{I} = \{t_k\}_{k=0}^{\infty}$ denote transmission time instants and R_k denote the data rate at time instant t_k. Then, $\{R_k\}_{k=0}^{\infty}$ forms a random process that characterizes stochastic variations on channel conditions. At each time instant t_k, the communication system can adjust its transmission power to send data through a wireless communication channel. Let $\Omega_p = \{1, 2, \ldots, M_p\}$ denote a finite set of transmission power levels with $i \in \Omega_p$ representing a power level i. The transmission power set is sorted in an ascending order such that larger numbers represent higher power levels. Let $p_k := p(t_k) \in \Omega_p$ denote the power level selected at time instant t_k. With the external environment modeled by a MDP, we define the SD-MC model below.

Definition 2.1: Given a power set Ω_p, a MDP $\mathcal{M}_{\text{env}}$ modeling the external environment, and a finite set of data rates $\mathcal{R} = \{r_1, r_2, \ldots, r_{M_R}\}$ that are arranged ascendingly, i.e., $r_i < r_j, \forall i < j$. Then, a wireless communication channel is said to be a SD-MC if $\forall s \in S, p \in \Omega_p$, and $\forall r_i, r_j \in \mathcal{R}$

$$\mathbb{P}\{R_{k+1} = r_i | R_k = r_j, s_k = s, p_k = p\} = P_{ij}(s, p) \tag{7}$$

where $P_{ij}(s, p)$ is a transition probability from data rate r_j to r_i under the transmission power p and environment state s.

The SD-MC model (7) extends the conventional finite state Markov model in the sense that the transition probabilities are defined as functions of transmission power and environment states [29], [30]. The intuition behind the SD-MC model is that a higher data rate is more likely to select if a high transmission power is applied and the environment state is controlled to ensure good channel conditions.

Different data rates are selected for each partitioned SNR to make sure that the BER is sufficiently small for the given SNR. In that regard, this article focuses on the aspect that the data rate is a more dominant factor than the packet loss in determining system stability and performance. Moreover, from information-theoretic perspective, the packet loss model is a special case of the proposed SD-MC model with one data rate $r = 0$ and the other $r = \infty$ [29].

III. Problem Formulation

Given the closed-loop NCS modeled in (5)–(7), Definition 3.1 formally states the *stochastic stability* notions considered in this article.

Definition 3.1 (Stochastic Stability [31]): Given the SD-MC model in (7) and the closed-loop NCS model in (5)–(6).

E The system is said to be ASE if there exist a class $\mathcal{KL}$ function $\beta(\cdot, \cdot)$ and a bounded set $\Omega_r = \{x \in \mathbb{R}^n : |x| < r\}$ such that for all $x_0 \in \Omega_r$, then

$$\mathbb{E}(|x(t)|) \leq \beta(|x_0|, t - t_0), \quad \forall t \in \mathbb{R}_{\geq 0} \tag{8}$$

and that $\lim_{t \to \infty} \mathbb{E}(|x(t)|) = 0$.

Authorized licensed use limited to: University of Houston. Downloaded on October 03,2022 at 15:45:04 UTC from IEEE Xplore. Restrictions apply.

P The system is said to be ASAS if $\forall \epsilon, t' > 0$, the following holds:

$$\mathbb{P}\left\{\lim_{t'\to\infty}\sup_{t\geq t'}|x(t)| \geq \epsilon\right\} = 0. \tag{9}$$

Remark 3.2: The ASAS is a stronger stability notion than that of the ASE in the sense that 1) the former implies the latter while 2) the latter normally does not lead to the former. Specifically, a system is ASAS if it is *exponentially stable in expectation*, i.e., there exists an exponential function $\beta(|x_0|, t-t_0) := c_1 \exp(-c_2(t-t_0))|x_0|$ with $c_i > 0, i = 1, 2$ such that inequality (8) holds [10], [32].

Problem 3.3 (Stability Problem): The first problem considered in this article is to design a MATI under which the NCS modeled in (5)–(6) under the proposed SD-MC model satisfies the stochastic stability notions in Definition 3.1.

Problem 3.4 (Codesign Problem): After solving the Problem 3.3 and obtaining the MATI, the second problem is to find optimal control and transmission power policies under which some predefined system specifications are optimized. Specifically, let μ_m and μ_p denote the control policy and transmission power policy, respectively. Then, for a given joint cost function $\{c(s,p,r)\}_{s\in S, p\in\Omega_p, r\in\mathcal{R}}$ the codesign problem is defined as that of finding an optimal policy $\mu^\star := (\mu_m^\star, \mu_p^\star)$ such that the average expected costs in (10) below are minimized under the obtained stability conditions

$$\begin{aligned} \min_{\mu_m,\mu_p} \quad & \lim_{\ell\to\infty}\frac{1}{\ell}\mathbb{E}_{s_0,R_0}^{\mu_m,\mu_p}\sum_{k=0}^{\ell} c(s_k,p_k,R_k) \\ \text{s.t.} \quad & \text{Stability conditions ensuring (8) or (9)} \end{aligned} \tag{10}$$

where s_0 and R_0 denote the initial states of the MDP system and the Markov channel, respectively.

IV. Main Results

Assumption 4.1 below is used to derive the main results.

Assumption 4.1 (see[27]): Consider the SHS in (5) and (6). Let $\overline{e} := [e; \xi]$ denote an augmented vector of the error states e and the size of the dynamic quantizer ξ. Suppose there exist

1) a function $W : \mathbb{N}_{\geq 0} \times \mathbb{R}^{n_e+1} \to \mathbb{R}_{\geq 0}$ that is locally Lipschitz with respect to $\overline{e}$
2) a function $V : \mathbb{R}^{n_x} \to \mathbb{R}_{\geq 0}$ that is locally Lipschitz, positive definite, and radially unbounded
3) a continuous function $H : \mathbb{R}^{n_x} \to \mathbb{R}_{\geq 0}$.

Assume further that there exist a finite set of constants $\{\lambda_i\}_{i=1}^{M_R}$, some real numbers $L \geq 0, \zeta > 0$, class $\mathcal{K}_\infty$ functions $(\underline{\alpha}_W, \overline{\alpha}_W, \underline{\alpha}_V, \overline{\alpha}_V) \in \mathcal{K}_\infty$, a continuous function $H : \mathbb{R}^{n_x} \to \mathbb{R}_{\geq 0}$, and a continuous positive definition function ϱ such that

1) $\forall k \in \mathbb{N}, \overline{e} \in \mathbb{R}^{n_x+1}$ and $r_i \in \mathcal{R} = \{r_1, \ldots, r_{M_R}\}$

$$\underline{\alpha}_W(|\overline{e}|) \leq W(k,\overline{e}) \leq \overline{\alpha}_W(|\overline{e}|) \tag{11a}$$

$$W(k+1, \overline{J}(k,\overline{e},r_i)) \leq \lambda_i W(k,\overline{e}) \tag{11b}$$

where $\overline{J}(k,\overline{e},r_i) = [J_e; J_\xi]$ with J_e and J_ξ are as in (6).

2) $\forall k \in \mathbb{N}, x \in \mathbb{R}^{n_x}$ and for almost all $\overline{e} \in \mathbb{R}^{n_x+1}$, then

$$\left\langle \frac{\partial W(k,\overline{e})}{\partial \overline{e}}, \overline{g}(x,\overline{e}) \right\rangle \leq LW(k,\overline{e}) + H(x) \tag{12}$$

where $\overline{g}(x,\overline{e}) = [g_e; g_\xi]$ with g_e and g_ξ are as in (5).

3) $\forall x \in \mathbb{R}^{n_x}$

$$\underline{\alpha}_V(x) \leq V(x) \leq \overline{\alpha}_V(x) \tag{13}$$

and $\forall k \in \mathbb{N}, \overline{e} \in \mathbb{R}^{n_x+1}$, and for almost all $x \in \mathbb{R}^{n_x}$, then

$$\begin{aligned} \langle \nabla V(x), \tilde{f}(x,e)\rangle \leq \varrho(|x|) - \varrho(W(k,\overline{e})) - H^2(x) \\ + \zeta^2 W^2(k,\overline{e}). \end{aligned} \tag{14}$$

Remark 4.2: Assumption 4.1 is similar to [33, Assumption 1], where the inequalities (11) of part 1) are used to characterize the bounds on the function of error states $\overline{e}$ as well as its growths for different data rates at discrete time instants. It is assumed that, for any given data rate $r_i \in \mathcal{R}$, there exists a corresponding positive real λ_i that bounds the growth of the error function from the above. The inequality (12) of part 2) assumes a linear growth of the error function in the continuous time domain. Inequalities (13) and (14) of part 3) are used to characterize the growth rate of the Lyapunov function with respect to the state x in the continuous time domain. The MATI bounds that ensure stochastic stability will be derived based on the parameters given in this assumption.

Under Assumption 4.1, sufficient conditions on the MATI that assure the ASE and ASAS of the SHS in (5)–(6) with SD-MC model in (7) are given in Theorems 4.3 and 4.5, respectively.

Theorem 4.3 (see[26]): Consider the SHS in (5)–(6), the SD-MC model in (7), and the controlled external environment $\mathcal{M}_{\text{env}}$. Suppose Assumption 4.1 holds, and let T_{MATI} denote the MATI. For a given joint policy $\mu = (\mu_m, \mu_p)$, the SHS is ASE if

$$T_{\text{MATI}} \leq \begin{cases} \frac{1}{L\eta}\arctan\left(\frac{\eta(1-\overline{\lambda})}{2\frac{\overline{\lambda}}{1+\overline{\lambda}}(\frac{\zeta}{L}-1)+1+\overline{\lambda}}\right) & \zeta > L \\ \frac{1}{L}\frac{1-\overline{\lambda}}{1+\overline{\lambda}} & \zeta = L \\ \frac{1}{L\eta}\operatorname{arctanh}\left(\frac{\eta(1-\overline{\lambda})}{2\frac{\overline{\lambda}}{1+\overline{\lambda}}(\frac{\zeta}{L}-1)+1+\overline{\lambda}}\right) & \zeta < L \end{cases} \tag{15}$$

with $\eta = \sqrt{|(\frac{\zeta}{L})^2 - 1|}$ and $\overline{\lambda}$ is a constant, which satisfies

$$\overline{\lambda} > \sqrt{\|\operatorname{diag}(\lambda_i^2)\overline{P}(\mu)\|} \tag{16}$$

where $\overline{P}(\mu) = [\overline{P}_{ij}(\mu)]_{1\leq i,j\leq M_R}$ with $\overline{P}_{ij}(\mu) = \sum_{p\in\Omega_p, s\in S}\mathbb{P}(r_i|r_j,s,p)\mathbb{P}(s,p|r_j)$.

Remark 4.4: The MATI bounds shown in (15) are functions of parameters ξ and L defined in Assumption 4.1, and $\overline{\lambda}$ that depends on the SD-MC model in (7). The proposed MATI bounds differ from the existing results in [10], [27], [32] in two aspects. First, the MATI bounds in (15) generalize the results in [27] as they take into account the impacts that the SD-MC channel has on the MATI. Such an impact is captured by the choice of parameter $\overline{\lambda}$ that must satisfies inequality (16). Existing results may thus be recovered from our MATI bounds by setting the parameter $\overline{\lambda}$ to be independent of the channel conditions. Second, the MATI results in this article extend our prior works in [10], [32] by considering a less conservative assumption on the system structure and a more general channel model.

Theorem 4.5 (see[26]): Suppose conditions (15) and (16) hold for the SHS in (5)–(6), and there exist positive constants $\underline{\alpha}_W, \overline{\alpha}_W, \underline{\alpha}_V, \overline{\alpha}_V$, and $\varrho > 0$ such that the conditions in (11), (13), and (14) in Assumption 4.1 hold with

$$\underline{\alpha}_W|\overline{e}| \leq W(k,\overline{e}) \leq \overline{\alpha}_W|\overline{e}| \tag{17a}$$

$$\underline{\alpha}_V|x|^2 \leq V(x) \leq \overline{\alpha}_V|x|^2 \tag{17b}$$

$$\begin{aligned} \left\langle \nabla V(x), \tilde{f}(x,e)\right\rangle \leq \varrho|x|^2 - \varrho W(k,\overline{e}) \\ - H^2(x) + \zeta^2 W^2(k,\overline{e}). \end{aligned} \tag{17c}$$

Then, the SHS in (5)–(6) is ASAS. ■

Proof: Please refer to [26] for the details of the proof.

With the stability results in Theorem 4.3, the codesign Problem 3.4 is formulated as a constrained optimization program with the stability condition in (16) as hard constraints.

Authorized licensed use limited to: University of Houston. Downloaded on October 03,2022 at 15:45:04 UTC from IEEE Xplore. Restrictions apply.

Theorem 4.6 below shows that, if stationary policies are considered, the codesign Problem 3.4 can be reformulated as a polynomial constrained program with a linear objective.

Theorem 4.6 (see[26]): Given the sets of MDP states S, transmission power Ω_p, and data rate $\mathcal{R}$, $\forall i, 1 \leq i \leq M_R$, let $X(s,r,p) \geq 0, \forall s, r, p$ denote the decision variables of the following CPOP:

$$\min_{\{X(s,r,p)\}} \quad \sum_{s\in S, p\in\Omega_p, r\in\mathcal{R}} c(r,s,p)X(s,r,p) \tag{18a}$$

$$\text{s.t.} \quad \sum_{s,p} X(s,r_i,p) - \sum_{p,s,r_j} P_{ij}(s,p)X(s,r_j,p) = 0, \ \forall r_i \in \mathcal{R} \tag{18b}$$

$$\sum_{s,p,r} X(s,r,p) = 1 \tag{18c}$$

$$\sum_{j=1}^{M_R} \sum_{s,p} P_{ij}(s,p)X(s,p) \prod_{\ell\neq j} X(r_\ell) - \theta_i^2 \prod_{j=1}^{M_R} X(r_j) \leq 0 \tag{18d}$$

where $X(s,p) = \sum_{j=1}^{M_R} X(s,r,p)$, [1] $X(r) = \sum_{s,p} X(s,r,p)$, $\theta_i = \overline{\lambda}/\lambda_i$, and $P_{ij}(s,p)$ is the transition probability of the SD-MC model in (7). Then, the optimal stationary power policy $\mu_p^\star = \{\mathbb{P}(p|r)\}_{p\in\Omega_p, r\in\mathcal{R}}$ and optimal probability distribution $\pi^\star = \{\mathbb{P}(s)\}_{s\in S}$ for the MDP states can be represented as

$$\mathbb{P}(p|r) = \frac{\sum_{s\in S} X^*(s,r,p)}{\sum_{p\in\Omega_p, s\in S} X^*(s,r,p)} \tag{19}$$

$$\mathbb{P}(s) = \sum_{p\in\Omega_p, r\in\mathcal{R}} X^*(s,r,p) \tag{20}$$

with $\{X^*(s,r,p)\}_{s\in S, r\in\mathcal{R}, p\in\Omega_p}$ is the solution of CPOP (18).

Remark 4.7: The inequality (18d) is equivalent to the stability condition in (16) if stationary policies are considered in the system. For all i with $1 \leq i \leq M_R$, let the following function h_i be those that form the inequality in (18d)

$$h_i(X) := \sum_{j=1}^{M_R} \sum_{s,p} P_{ij}(s,p)X(s,p) \prod_{\ell\neq j} X(r_\ell) - \theta_i^2 \prod_{j=1}^{M_R} X(r_j)$$

It is clear that functions $\{h_i\}_{1\leq i\leq M_R}$ are polynomial functions whose orders are determined by the number of data rates, M_R. The solutions to the CPOP (18) thus represent the occupation measures of the data rates, MDP states, and transmission power. These measures are used to construct the optimal power policy that is conditioned on the data rate r. One can refine the power policy using the optimal occupation measures $\{X^*(s,r,p)\}$ by defining it to be conditional on both data rate r and the environment state s. Specifically, $\mathbb{P}(p\,|\,r,s) = X^*(s,r,p)/\sum_{p\in\Omega_p, s\in S} X^*(s,r,p)$ where the power policy needs to use both data rate and MDP state to determine the probability of choosing a power level. In cases where environment state s may not be available to the communication system, the power policy $\mathbb{P}(p\,|\,r)$ is practically more feasible to implement than $\mathbb{P}(p\,|\,r,s)$.

Note that it is in general computationally hard (NP hard) to even decide whether a polynomial with degree equal to or greater than three is convex over a compact region [35]. Such a negative result on CPOP decidability suggests that the structure of the polynomial constraints in (18) must be investigated to have efficient solutions. In Section IV-A1, we show that the CPOP formulated in (18) can be reduced to a quadratic constraint programming problem (QCPP) for the case of two-state SD-MC. The two-state SD-MC can be considered as a generalization of the well known bursty erasure channel [29]. For the general case of SD-MC channels, we propose a LP method in Section IV-A2 to approximate the solutions of the CPOP (18).

1) Two-State SD-MC: Quadratic Constraint Programs: This section considers a two-state SD-MC that has only two data rates.

For this model, Lemma 4.8 shows that the polynomial constraints in (18d) are reduced to quadratic constraints. The CPOP (18) thus is a QCPP which can be solved by semidefinite programming (SDP) methods if the matrices associated with the corresponding quadratic constraints are positive semidefinite.

Lemma 4.8: Consider a two-state SD-MC with data rates of r_1 and r_2. Given the MDP state set S and transmission power set Ω_p, the polynomial constraints in (18d) are quadratic constraints, which can be formulated as

$$X^T \overline{Q}_1 X \leq 0 \tag{21}$$

$$X^T \overline{Q}_2 X \leq 0 \tag{22}$$

where $X = [X(r_1,s_1,p_1), X(r_1,s_1,p_2), \ldots, X(r_1,s_2,p_1), \ldots, X(r_2,s_{M_s},p_{M_p})]^T$ is an augmented vector whose elements are arranged in the order of transmission power p, MDP state s, and data rate r. Matrices $\overline{Q}_1, \overline{Q}_2 \in \mathbb{R}^{2M_sM_p\times 2M_sM_p}$ are of the forms

$$\overline{Q}_1 = A_{11}^T I_1 + A_{12} I_2 - \theta_1^2 I_2^T I_1$$

$$\overline{Q}_2 = A_{21}^T I_1 + A_{22} I_2 - \theta_2^2 I_2^T I_1$$

where $A_{ij} = [\vec{P}_{ij}, \vec{P}_{ij}]_{1\times 2M_sM_p}$ with $\vec{P}_{ij} = Vec(P_{ij}), \forall i,j \in \{1,2\}$, $\theta_i = \overline{\lambda}/\lambda_i$ with $i = 1,2$, $I_1 = [\mathbf{0}, \mathbf{e}]$, and $I_2 = [\mathbf{e}, \mathbf{0}]$, in which $\mathbf{0}$ and $\mathbf{e}$ are row vectors of M_s and M_p of zeros and ones, respectively.

Proof: The proof is provided in Appendix VII. ■

Based on Lemma 4.8, Theorem 4.9 below shows that the resulting QCPP can be solved via SDP.

Theorem IV.9: Consider a two-state SD-MC and suppose $\overline{Q}_1, \overline{Q}_2 \succeq 0$ hold for the matrices in the quadratic constraints (21) and (22). Then, the CPOP in (18) can be solved using SDP methods.

Proof: The proof is straightforward from the fact that constraints in (21) and (22) are convex if matrices $\overline{Q}_1, \overline{Q}_2$ are positive semidefinite (i.e., $\overline{Q}_1, \overline{Q}_2 \succeq 0$) ■

2) Linear Programming Relaxations: This section presents a LP relaxation of the CPOP (18) by applying the 1-norm form on the stability condition derived in (16). Specifically, Theorem 4.10 below shows that both the ASE and ASAS properties can be attained under a conservative T_{MATI} that is induced by a 1-norm condition. Proposition 4.12 subsequently proves that such a condition leads to linear constraints in the formulated optimization problem.

Theorem 4.10: Consider the SHS (5)–(6), the SD-MC model (7), and the controlled external environment $\mathcal{M}_{\text{env}}$. Suppose the T_{MATI} is defined by condition (15) for some constant $\overline{\lambda} \in \mathbb{R}_+$ that satisfies

$$\overline{\lambda} > \sqrt{M_R \| \operatorname{diag}(\lambda_i^2)\overline{P}(\mu)\|_1}. \tag{23}$$

Then the SHS (5)–(6) is ASE if Assumption 4.1 holds. Furthermore, system (5)–(6) is ASAS if condition (17) holds.

Proof: The proof is straightforward by the condition between ∞-norm and 1-norm. Specifically, $\| \operatorname{diag}(\lambda_i^2)\overline{P}(\mu)\| \leq M_R \| \operatorname{diag}(\lambda_i^2)\overline{P}(\mu)\|_1$ due to $\|A\| \leq n\|A\|_1, \forall A \in \mathbb{R}^{m\times n}$, then $\forall \overline{\lambda} > 0$ we have

$$\overline{\lambda} > \sqrt{M_R \| \operatorname{diag}(\lambda_i^2)\overline{P}(\mu)\|_1} \geq \sqrt{\| \operatorname{diag}(\lambda_i^2)\overline{P}(\mu)\|}.$$

[1] $X(A)$ denote the occupation (probability) measure [34] that assigns a probability to the event A

Authorized licensed use limited to: University of Houston. Downloaded on October 03,2022 at 15:45:04 UTC from IEEE Xplore. Restrictions apply.

The above inequalities imply that the satisfaction of the 1-norm condition in (23) leads to stability conditions in (16) that are shown to ensure ASE as proven in Theorem 4.3 and ASAS in Theorem 4.5. Thus, the proof is complete. ■

Remark 4.11: The use of stability constraints (23) in the codesign problem essentially trades the optimality with computational efficiency. Regarding the system optimality, the constrained optimization problem with constraints (23) leads to suboptimal solutions because stability constraints in (23) are more conservative than polynomial constraints in (16). Specifically, the size of the sets formed by constraints in (23) is inversely proportional to the number of data rates M_R. Nevertheless, the use of constraints (23) reduces the original NP-hard CPOP to more computationally tractable LP problems as stated in Proposition 4.12 below.

Proposition 4.12: For a given $\overline{\lambda} \in \mathbb{R}_+$, let $\mathcal{H}_\mu$ denote a set of joint policies $\mu = (\mu_m, \mu_p)$ satisfying the ∞-norm stability condition in (16), and let $\mathcal{H}_{\tilde{\mu}}$ denote a set of joint policies $\tilde{\mu} = (\tilde{\mu}_m, \tilde{\mu}_p)$ that satisfy the 1-norm stability condition in (23). Then

1) $\mathcal{H}_{\tilde{\mu}} \subset \mathcal{H}_\mu$.
2) with the 1-norm stability condition (23), the inequalities in (18d) of the CPOP (18) are linear inequalities.
3) let $\mu^\star$ and $J^\star$ denote the optimal joint policy and cost, respectively, of the optimization problem (10) with the ∞-norm stability condition. Let $\tilde{\mu}^\star$ and $\tilde{J}^\star$ denote the optimal joint policy and cost, respectively, under the 1-norm stability condition. Then $J^\star \leq \tilde{J}^\star$.

Proof: The proof is in included in Appendix VII. ■

After the optimal power policy $\mu_p^\star = \{\mathbb{P}(p|r)\}_{p\in\Omega_p, r\in\mathcal{R}}$ and stationary distribution for MDP states $\pi^\star = \{\mathbb{P}(s)\}_{s\in S}$ are obtained from Theorem 4.6, the next step is to find a control policy $\mu_m = \{\mathbb{P}(a|s)\}_{a\in A(s), s\in S}$ that achieves the optimal stationary distribution $\pi^\star$. Let $\{c_m(s,a)\}_{s\in S, a\in A}$ denote the cost function for each state-action pair of the MDP process. Then, the optimal control policy $\mu_m^\star$ can be obtained by solving the optimization in Problem 4.13 below.

Problem 4.13: Let $\mathcal{M}_{\text{env}} = \{S, s_0, A, Q\}$ be an ergodic MDP with a desired stationary distribution $\pi^\star$ that is obtained by solving the optimization problem (18). The objective is to find an optimal control policy $\mu_m^\star$ that solves the following optimization while attaining the desired stationary distribution $\pi^\star$:

$$\min_{\mu_m} \lim_{T\to\infty} \frac{1}{T} \mathbb{E}_{s_0}^{\mu_m} \left[\sum_{i=0}^{T} c_m(s_k, a_k) \right] \tag{24a}$$

$$\text{s.t. } Q(\mu_m)\pi^\star = \pi^\star \tag{24b}$$

where $Q(\mu_m)$ is the transition matrix of the Markov chain induced by the control policy μ.

Theorem 4.14 below shows that Problem 4.13 can be formulated and efficiently solved using LP methods.

Theorem 4.14 (see[26]): For a given $\pi^\star = [\pi^\star(s_1), \ldots, \pi^\star(s_{M_s})]^T$ with $\pi^\star(s)$ being the probability distribution of the state $s \in S$, let $\{Y(s,a)\}_{s\in S, a\in A}$ denote the decision variables of LP problem as follows:

$$\min_{\{Y(s,a)\}} \quad \sum_{s\in S, a\in A} c_m(s,a) Y(s,a) \tag{25a}$$

$$\text{s.t.} \quad \sum_a Y(s,a) - \sum_{s',a} q(s|s',a) Y(s',a) = 0, \forall s \in S \tag{25b}$$

$$\sum_{s\in S, a\in A} Y(s,a) = 1, \quad Y(s,a) \geq 0, \forall s, a \tag{25c}$$

$$\sum_{a\in A} Y(s,a) = \pi^\star(s), \forall s \in S. \tag{25d}$$

Then, the corresponding optimal control policy $\mu_m^\star$ for Problem (24) can be obtained by

$$\mathbb{P}(a|s) = \frac{Y^*(s,a)}{\sum_{a\in A} Y^*(s,a)}, \quad \forall s \in S, a \in A \tag{26}$$

where $\{Y^*(s,a)\}$ is the solution to the LP problem in (25).

V. Simulation Results

This section presents an industrial example of a nonlinear robotic arm and a forklift vehicle to verify the given results on stochastic stability (see Theorem 4.5) and optimal codesign policy proposed in Theorems 4.9 and 4.10.

The dynamics of a nonlinear single link robotic arm is modeled as $\dot{x}_1 = x_2, \dot{x}_2 = -4.905\sin(x_1) + 2u$, where x_1 and x_2 are the arm's angle and rotational velocities, respectively, and u is the input torque. The objective of the robotic arm is to track a predefined trajectory generated by a reference system as $\dot{x}_{1d} = x_{2d}, \dot{x}_{2d} = -4.905\sin(x_{1d}) + 2u_{ff}$, where $x_{id}, i = 1, 2$ are the reference angle and rotational velocities, respectively, and $u_{ff} = 10\sin(50t)$ is the input signal to the reference system. We assume that the states of the reference system $x_{id}, i = 1, 2$ as well as the input signal u_{ff} are available to the remote controller. Following the design policy in (4), the model-based controller can thus be constructed as $\dot{\hat{x}}_1 = \hat{x}_2, \dot{\hat{x}}_2 = -4.905\sin(\hat{x}_1) + 2u, u = 2^{-1}(4.905(\sin(\hat{x}_1) - \sin(x_{1d})) - (\hat{x}_1 - x_{1d}) - (\hat{x}_2 - x_{2d})) + u_{\text{ff}}$. Let $\bar{x} = x - x_d$ with $x = [x_1, x_2]^T$ and $x_d = [x_{1d}, x_{2d}]^T$ denote the tracking error, and define the error states $e = \bar{x} - \hat{\bar{x}} = x - \hat{x}$ with $\hat{\bar{x}} = \hat{x} - x_d$. Then, the dynamics of e and ξ can be written as $\dot{e} = [e_2; -4\cos\frac{2x_1 - e_1}{2}\sin\frac{e_1}{2}]$ and $\dot{\xi} = 2\xi$.

The dynamics of a forklift vehicle is abstracted as a two-state MDP with a state set of $\{s_1, s_2\}$ with s_1 representing the shadow fading region and s_2 the nonshadow fading region. The vehicle is able to take an action from the set $\{\text{Go}, \text{Stay}\}$ to make transitions between regions. The transition probabilities of the states under each action are $\mathbb{P}\{s_1|s_1, \text{Stay}\} = \mathbb{P}\{s_2|s_2, \text{Stay}\} = 0.9$ and $\mathbb{P}\{s_1|s_1, Go\} = \mathbb{P}\{s_2|s_2, Go\} = 0.1$. Their associated costs are $c_m(s_1, \text{Stay}) = c_m(s_1, Go) = 0.4$ and $c_m(s_2, \text{Stay}) = c_m(s_2, Go) = 0.6$. The costs are selected to simulate scenarios where the interests of moving vehicle are in conflict with the robotic networked arm system (i.e., the shadow-fading state s_1 is assigned a lower cost than the nonshadow fading state s_2). Such scenarios represent challenging situations that are commonly encountered in complex industrial environments where cooperative and adaptive strategies are needed the most. Under the two-state MDP, a two-state SD-MC model is constructed to simulate the *state-dependent* fading channel for the robotic arm. The data rates of the two-state SD-MC are $r_1 = 0$ and $r_2 = 2$, and a two-level transmission power set $\{H, L\}$ is selected with H and L representing the high and low level, respectively. The state-dependent transition probabilities under different MDP states and transmission power are $P_{11}(s_1, L) = P_{21}(s_1, L) = 0.8, P_{11}(s_1, H) = P_{21}(s_1, H) = 0.6, P_{11}(s_2, L) = 0.4, P_{11}(s_2, H) = P_{21}(s_2, H) = 0.1, P_{21}(s_2, L) = 0.5$. The power costs are $c_p(H) = 0.6, c_p(L) = 0.4$ and the costs for the data rates are $c_r(r_1) = 0.6, c_r(r_2) = 0.4$.

Let $W(e) = |e|$, and the parameters $L = 4.905, \zeta = \sqrt{2}, \lambda_0 = 1, \lambda_1 = 0.5$ are selected to satisfy Assumption 4.1. From (15) in Theorem 4.5, the MATI can be determined as $T_{\text{MATI}} = 0.072\,s$ for $\overline{\lambda} > \sqrt{\|\operatorname{diag}(\lambda_i^2)\overline{P}(\mu)\|} = 0.6325$ with $\overline{P}(\mu) = [0.2, 0.2; 0.8, 0.8]$, and $T = 0.07\,s \leq$ MATI. Fig. 2 shows that the maximum (blue dashed lines) and minimum (red dash-dot lines) trajectories evaluated over 1000 runs under $T = 0.07\,s$, asymptotically converge to the origin, which implies ASAS (see Theorem 4.5). Fig. 3 shows the comparison

Authorized licensed use limited to: University of Houston. Downloaded on October 03,2022 at 15:45:04 UTC from IEEE Xplore. Restrictions apply.

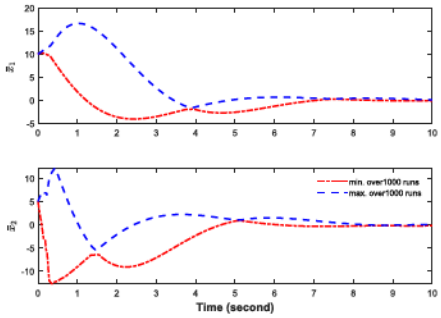

Fig. 2. Maximum and minimum values for the state trajectories of a networked robotic arm with $T = 0.07\,s$.

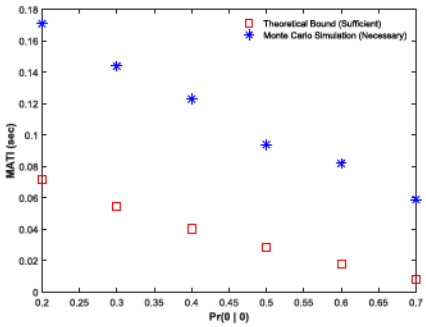

Fig. 3. Comparison of sufficient and necessary bounds on MATI under different channel conditions $\mathbb{P}\{r' = 0|r = 0\} = 0.2, 0.3, 0.4, 0.5, 0.6, 0.7$.

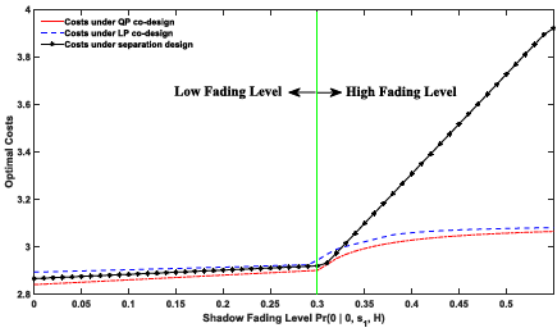

Fig. 4. Performance comparison of the proposed codesign method against the separation method under a wide range of channel conditions ranging from 0 to 0.55.

of sufficient bounds (marked by red squares) on MATI derived in (15) against the necessary bounds (marked by blue stars) generated by Monte Carlo simulations that gradually increase the transmission interval T until the system is *almost surely asymptotically unstable*. The comparison results show that the sufficient bounds are around 2–8 times smaller than the necessary bounds over a wide range of channel conditions (a variety of conditions are simulated by selecting different transition probabilities $\mathbb{P}(0\,|\,0)$). The gap is reasonably close given the fact that similar conservativeness were also reported in [36] for deterministic systems.

This article also compares the optimal co-design strategies proposed in Theorems 4.6–4.10 against traditional separation design methods (e.g., [21]), where the design of optimal power policies is independent of the control policy design. Fig. 4 shows the comparison results of optimal joint costs generated by the separation design method (marked by a black solid-dotted line) and the codesign strategy (the QCPP result is marked by a red dotted line, while the LP result is marked by a blue dash line) over a wide range of shadow fading levels. As shown in the plots, the QCPP-based codesign method leads to lowest costs across the whole range of the shadow fading among all three strategies. Interestingly, codesign strategies under both quadratic and LM are more robust in the high shadow fading regime (i.e., the region between 0.3 and 0.55) than that of the separation design, in the sense that the optimal cost curves under the former two are relatively flat regardless of the fading levels, while that based on the separation design method linearly increases as the fading level is increased.

VI. Conclusion

This article presented a codesign paradigm to ensure both stochastic stability and optimal performance of industrial NCSs under *state-dependent fading channels*. A novel SD-MC model was proposed to characterize the correlation between channel conditions and external environments. The proposed channel model was used to derive sufficient conditions on MATI that ensure ASE and ASAS properties of the industrial NCS. With the derived stability conditions as constraints, the codesign problem was reformulated as CPOP that can be either solved by semidefinite programs under a two-state Markov channel, or approximated by LP with suboptimal solutions under the general Markov channel. Simulation results of a nonlinear robotic arm and a forklift vehicle in industrial settings were provided to verify the efficacy of proposed approaches.

Appendix

Proof of Lemma 4.8: Consider the polynomial constraint in (18d) with a two-state SD-MC (i.e., $M_R = 2$). Then, the polynomial inequality (18d) is reduced to

$$\sum_{j=1}^{2}\sum_{s,p} P_{ij}(s,p)X(s,p)\prod_{\ell\neq j} X(r_\ell) \le \theta_i^2 \prod_{j=1}^{2} X(r_j), \forall i = 1,2$$

$$\iff \sum_{s,p} P_{i1}(s,p)X(s,p)X(r_2) + \sum_{s,p} P_{i2}(s,p)X(s,p)X(r_1)$$

$$\le \theta_i^2 X(r_1)X(r_2), \forall i = 1,2. \tag{27}$$

The order of the polynomial terms in (27) is 2, which makes it a quadratic constraint. Let $X = [X(r_1, s_1, p_1), \ldots X(r_2, s_1, p_1), \ldots, X(r_2, s_{M_s}, p_{M_p})]^T$ denote a column vector with $M_s = |S|$ and $M_p = |\Omega_p|$ being the sizes of the MDP state set and transmission power set, respectively. Let $I_1 = [\mathrm{e}, 0]$, $I_2 = [0, \mathrm{e}]$ with $0_{1\times M_s M_p}$ and $\mathrm{e}_{1\times M_s M_p}$ denote the row vectors of $M_s M_p$ zeros and ones, respectively. Let $\vec{P}_{ij} = Vec(P_{ij}) = [P_{ij}(s_1,p_1), P_{ij}(s_2,p_1), \ldots, P_{ij}(s_{M_s},p_1), \ldots, P_{ij}(s_{M_s},p_{M_p})]$ denote the vectorization of the matrix $P_{ij}, \forall i,j = 1,2$. Then, with $X(r_1) = I_1 X$ and $X(r_2) = I_2 X$, the constraint in (27) becomes

$$X^T \begin{bmatrix} \vec{P}_{i1}^T \\ \vec{P}_{i1}^T \end{bmatrix} I_2 X + x^T \begin{bmatrix} \vec{P}_{i2}^T \\ \vec{P}_{i2}^T \end{bmatrix} I_1 X - \theta_i^2 I_1 X I_2 X \le 0, \forall i = 1,2$$

$$\iff X^T \left(\underbrace{\begin{bmatrix} \vec{P}_{i1}^T \\ \vec{P}_{i1}^T \end{bmatrix} I_2 + \begin{bmatrix} \vec{P}_{i2}^T \\ \vec{P}_{i2}^T \end{bmatrix} I_1 - \theta_i^2 I_1^T I_2}_{\overline{Q}_i} \right) X \le 0, \forall i = 1,2.$$

The proof is then complete. ■

Proof of Proposition 4.12: Properties 1) and 3) hold due to the fact that for any joint-policies μ satisfying the 1-norm constraint in (23) guarantee that the ∞-norm stability condition (16) is satisfied. This

Authorized licensed use limited to: University of Houston. Downloaded on October 03,2022 at 15:45:04 UTC from IEEE Xplore. Restrictions apply.

implies that the feasible set of the joint policies $\mathcal{H}_{\tilde{\mu}}$ induced by the 1-norm stability constraint in (23) is strictly smaller than the one $\mathcal{H}_{\mu}$ generated by the ∞-norm condition in (16). Therefore, the optimal costs J^* under the set $\mathcal{H}_{\mu}$ are clearly smaller than the optimal costs under the set $\mathcal{H}_{\tilde{\mu}}$. To prove property 2), consider the 1-norm condition as follows:

$$\begin{aligned}
&\overline{\lambda} > \sqrt{M_R \| \operatorname{diag}(\lambda_i^2)\overline{P}(\mu)\|_1} \\
\iff &\| \operatorname{diag}(\lambda_i^2)\overline{P}(\mu)\|_1 < \left(\frac{\overline{\lambda}}{M_R}\right)^2 \\
\iff &\sum_{i=1}^{M_R} \lambda_i^2 \sum_{s,p} P_{ij}(s,p)\mathbb{P}(s,p\,|\,r_j) < \left(\frac{\overline{\lambda}}{M_R}\right)^2, \forall j \\
\iff &\sum_{i=1}^{M_R} \lambda_i^2 \sum_{s,p} P_{ij}(s,p)\frac{\sum_{r_j} X(s,p,r_j)}{\sum_{s,p} X(s,p,r_j)} < \left(\frac{\overline{\lambda}}{M_R}\right)^2, \forall j. \quad (28)
\end{aligned}$$

Multiplying $\sum_{s,p} X(s,p,r_j)$ on both sides of the inequality in (28) implies for all j that

$$\sum_{i=1}^{M_R} \lambda_i^2 \sum_{s,p} P_{ij}(s,p) \sum_{r_j} X(s,p,r_j) < \sum_{s,p} X(s,p,r_j)\left(\frac{\overline{\lambda}}{M_R}\right)^2.$$

The above inequality shows that the 1-norm stability conditions in (23) are linear constraints. Hence, the optimization problem in (10) is a LP under the relaxed 1-norm stability conditions. ■

REFERENCES

[1] S. Wang, J. Wan, D. Li, and C. Zhang, "Implementing smart factory of industrie 4.0: An outlook," *Int. J. Distrib. Sens. N.*, vol. 12, no. 1, 2016, Art. no. 3159805.

[2] A. Ahlén *et al.*, "Toward wireless control in industrial process automation: A case study at a paper mill," *IEEE Control Syst. Mag.*, vol. 39, no. 5, pp. 36–57, Oct. 2019.

[3] P. Agrawal, A. Ahlén, T. Olofsson, and M. Gidlund, "Long term channel characterization for energy efficient transmission in industrial environments," *IEEE Trans. Commun.*, vol. 62, no. 8, pp. 3004–3014, Aug. 2014.

[4] F. Qin *et al.*, "Link quality estimation in industrial temporal fading channel with augmented Kalman filter," *IEEE Trans. Industr. Inform.*, vol. 15, no. 4, pp. 1936–1946, Apr. 2019.

[5] D. E. Quevedo, A. Ahlen, and K. H. Johansson, "State estimation over sensor networks with correlated wireless fading channels," *IEEE Trans. Autom. Control*, vol. 58, no. 3, pp. 581–593, Mar. 2013.

[6] S. Kharb and A. Singhrova, "A survey on network formation and scheduling algorithms for time slotted channel hopping in industrial networks," *J. Netw. Comput. Appl.*, vol. 126, pp. 59–87, 2019.

[7] R. T. Hermeto, A. Gallais, and F. Theoleyre, "Scheduling for IEEE802.15.4-TSCH and slow channel hopping MAC in low power industrial wireless networks: A survey," *Comput. Commun.*, vol. 114, pp. 84–105, 2017.

[8] D. E. Quevedo, J. Østergaard, and A. Ahlen, "Power control and coding formulation for state estimation with wireless sensors," *IEEE Trans. Control Syst. Technol.*, vol. 22, no. 2, pp. 413–427, Mar. 2014.

[9] Y. Z. Lun, C. Rinaldi, A. Alrish, A. D'Innocenzo, and F. Santucci, "On the impact of accurate radio link modeling on the performance of wirelesshart control networks," in *Proc. IEEE INFOCOM*, 2020, pp. 2430–2439.

[10] B. Hu, Y. Wang, P. V. Orlik, T. Koike-Akino, and J. Guo, "Co-design of safe and efficient networked control systems in factory automation with state-dependent wireless fading channels," *Automatica*, vol. 105, pp. 334–346, 2019.

[11] T. Olofsson, A. Ahlen, and M. Gidlund, "Modeling of the fading statistics of wireless sensor network channels in industrial environments," *IEEE Trans. Signal Process.*, vol. 64, no. 12, pp. 3021–3034, Jun. 2016.

[12] M. Eriksson and T. Olofsson, "On long-term statistical dependences in channel gains for fixed wireless links in factories," *IEEE Trans. Commun.*, vol. 64, no. 7, pp. 3078–3091, Jul. 2016.

[13] E. Vinogradov, W. Joseph, and C. Oestges, "Measurement-based modeling of time-variant fading statistics in indoor peer-to-peer scenarios," *IEEE Trans. Antennas Propag.*, vol. 63, no. 5, pp. 2252–2263, May 2015.

[14] A. J. Goldsmith and S.-G. Chua, "Variable-rate variable-power MQAM for fading channels," *IEEE Trans. Commun.*, vol. 45, no. 10, pp. 1218–1230, Oct. 1997.

[15] Y. Ma, C. Lu, and Y. Wang, "Efficient holistic control: Self-awareness across controllers and wireless networks," *ACM Trans. Cyber- Phys. Syst.*, vol. 4, no. 4, pp. 1–27, 2020.

[16] H. Zhang and W. X. Zheng, "Denial-of-service power dispatch against linear quadratic control via a fading channel," *IEEE Trans. Autom. Control*, vol. 63, no. 9, pp. 3032–3039, Sep. 2018.

[17] M. Rabi, C. Ramesh, and K. H. Johansson, "Separated design of encoder and controller for networked linear quadratic optimal control," *SIAM J. Control Optim.*, vol. 54, no. 2, pp. 662–689, 2016.

[18] G.D. Girolamo and A. D'Innocenzo, "Codesign of controller, routing & scheduling in wirelesshart networked control systems," *Int. J. Robust Nonlinear Control*, vol. 29, no. 7, pp. 2171–2187, 2019.

[19] C. Peng and T. C. Yang, "Event-triggered communication and $\mathcal{H}_\infty$ control co-design for networked control systems," *Automatica*, vol. 49, no. 5, pp. 1326–1332, 2013.

[20] G. Zhao, M. A. Imran, Z. Pang, Z. Chen, and L. Li, "Toward real-time control in future wireless networks: Communication-control co-design," *IEEE Commun. Mag.*, vol. 57, no. 2, pp. 138–144, Feb. 2019.

[21] K. Gatsis, A. Ribeiro, and G. J. Pappas, "Optimal power management in wireless control systems," *IEEE Trans. Autom. Control*, vol. 59, no. 6, pp. 1495–1510, Jun. 2014.

[22] X. Ren, J. Wu, K. H. Johansson, G. Shi, and L. Shi, "Infinite horizon optimal transmission power control for remote state estimation over fading channels," *IEEE Trans. Autom. Control*, vol. 63, no. 1, pp. 85–100, Jan. 2018.

[23] A. S. Leong and D. E. Quevedo, "Kalman filtering with relays over wireless fading channels," *IEEE Trans. Autom. Control*, vol. 61, no. 6, pp. 1643–1648, Jun. 2016.

[24] J. Chakravorty and A. Mahajan, "Remote estimation over a packet-drop channel with markovian state," *IEEE Trans. Autom. Control*, vol. 65, no. 5, pp. 2016–2031, May 2020.

[25] D. Dolz, D. Quevedo, I. Peñarrocha, A. Leong, and R. Sanchis, "Co-design of jump estimators & transmission policies for wireless multi-hop networks with fading channels," *Automatica*, vol. 81, pp. 68–74, 2017.

[26] B. Hu and T. A. Tamba, "Optimal networked control systems with state-dependent Markov channels," in *Proc. Amer. Control Conf.*, 2021, pp. 2707–2712.

[27] D. Nesic, A. R. Teel, and D. Carnevale, "Explicit computation of the sampling period in emulation of controllers for nonlinear sampled-data systems," *IEEE Trans. Autom. Control*, vol. 54, no. 3, pp. 619–624, Mar. 2009.

[28] D. Nesic and D. Liberzon, "A unified framework for design and analysis of networked and quantized control systems," *IEEE Trans. Autom. Control*, vol. 54, no. 4, pp. 732–747, Apr. 2009.

[29] P. Minero, L. Coviello, and M. Franceschetti, "Stabilization over Markov feedback channels: The general case," *IEEE Trans. Autom. Control*, vol. 58, no. 2, pp. 349–362, Feb. 2013.

[30] Q. Zhang and S. A. Kassam, "Finite-state Markov model for Rayleigh fading channels," *IEEE Trans. Commun.*, vol. 47, no. 11, pp. 1688–1692, Nov. 1999.

[31] R. Khasminskii, *Stochastic Stability of Differential Equations*. Berlin/Heidelberg, Germany: Springer Science & Business Media, 2011, vol. 66.

[32] B. Hu and T. A. Tamba, "Optimal codesign of industrial networked control systems with state-dependent correlated fading channels," *I. J. Robust Nonlinear Control*, vol. 29, no. 13, pp. 4472–4493, 2019.

[33] D. Carnevale, A. R. Teel, and D. Nesic, "A Lyapunov proof of an improved maximum allowable transfer interval for networked control systems," *IEEE Trans. Autom. Control*, vol. 52, no. 5, pp. 892–897, May 2007.

[34] E. Altman, *Constrained Markov Decision Processes*. Boca Raton, FL, USA: CRC Press, 1999, vol. 7.

[35] A. A. Ahmadi and G. Hall, "On the complexity of detecting convexity over a box," *Math. Prog.*, vol. 182, no. 1, pp. 429–443, 2020.

[36] D. Nesic and A. R. Teel, "Input-output stability properties of networked control systems," *IEEE Trans. Autom. Control*, vol. 49, no. 10, pp. 1650–1667, Oct. 2004.

Authorized licensed use limited to: University of Houston. Downloaded on October 03,2022 at 15:45:04 UTC from IEEE Xplore. Restrictions apply.